

POLYCHROMATIC SIMULTANEOUS WDXRF FOR VALENCE EVALUATION OF CATHODE ACTIVE MATERIALS IN LITHIUM-ION BATTERIES

Tetsuya Yoneda¹, Takuro Izumi¹, Satoshi Tokuda¹, Susumu Adachi¹, Kenji Sato¹,
Misako Kobayashi², Takashi Mukai², Hideaki Tanaka², and Masahiro Yanagida²

¹ Shimadzu Corporation, Kyoto, Japan

² National Institute of Advanced Industrial Science and Technology (AIST), Osaka, Japan

ABSTRACT

Polychromatic simultaneous wavelength-dispersive X-ray fluorescence (PS-WDXRF) achieves high-energy resolution. The measured energy-identification precision is approximately 20 meV. The precision is sufficient for the valence state evaluation of lithium ion battery (LIB) cathodes through the peak shifts of X-ray fluorescence lines. Ex-situ cathode material measurement was performed with PS-WDXRF; the valence state of manganese cathode material changed from approximately 3.9 at the charged state to 3.5 at the discharged state, which is in good accordance with the electrochemical reaction formula.

INTRODUCTION

For the development of lithium-ion batteries (LIBs), cathode materials are being improved to achieve higher energy capacity, especially manganese-based cathode active materials because they are inexpensive. Analyzing the valence state of the cathode active material during charge and discharge cycles is a practical approach towards understanding the redox mechanism that may help in defining materials to achieve higher energy capacity. Valence state evaluations are typically performed using X-ray absorption fine structure (XAFS) measurements with a synchrotron X-ray source. Although this method is conventionally applied to cathode evaluation, it is difficult to define the accurate valence state. To conduct high-precision in-house analyses, we have developed a polychromatic simultaneous wavelength-dispersive X-ray fluorescence (PS-WDXRF) spectrometer (Sato *et al.*, 2017).

This document was presented at the Denver X-ray Conference (DXC) on Applications of X-ray Analysis.

Sponsored by the International Centre for Diffraction Data (ICDD).

This document is provided by ICDD in cooperation with the authors and presenters of the DXC for the express purpose of educating the scientific community.

All copyrights for the document are retained by ICDD.

Usage is restricted for the purposes of education and scientific research.

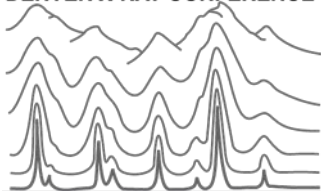
DXC Website

– www.dxcicdd.com

ICDD Website

- www.icdd.com

DENVER X-RAY CONFERENCE®



The PS-WDXRF spectrometer comprises of an X-ray tube, a slit, a flat Ge (220) crystal, and a 1280-channel silicon strip position-sensitive detector (SSD), which is Dectris Mythen2 R 1K. The X-rays dispersed by the crystal are simultaneously detected by the SSD, and the detected signals at each channel provide intensity information at each energy. This is because the X-ray whose wavelength meets Bragg's law at one position of the crystal reaches the channel of the SSD whose position corresponds to the position of the crystal. The optical configuration is depicted in Figure 1. There are no movable parts in the optical setup. The developed PS-WDXRF is designed for detecting X-rays in the range of 5.38 – 6.52 keV, which is designed for chemical analysis of manganese. The relationship between the SSD channel and X-ray energy was calculated with a geometrical equation (Sato *et al.*, 2017), and then this converted energy value was applied to obtained spectra. Figure 2 shows the obtained spectra that were fitted with Lorentzian functions via the least square algorithm. The optical geometry allows one to clearly distinguish between the Fe $K\alpha_1$ line around 6.40 keV and the Fe $K\alpha_2$ line around 6.39 keV, and also to achieve an energy resolution of 3.9 eV (FWHM: full width at the half maximum) at the Fe $K\alpha_1$ line. This is obviously higher than the resolution of 10 to 30 eV of conventional WDXRF spectrometers. This study using PS-WDXRF demonstrates the performance of the energy-identification precision, the availability of valence estimation, and the results applied to valence evaluation of actual LIB cathodes with different state of charge.

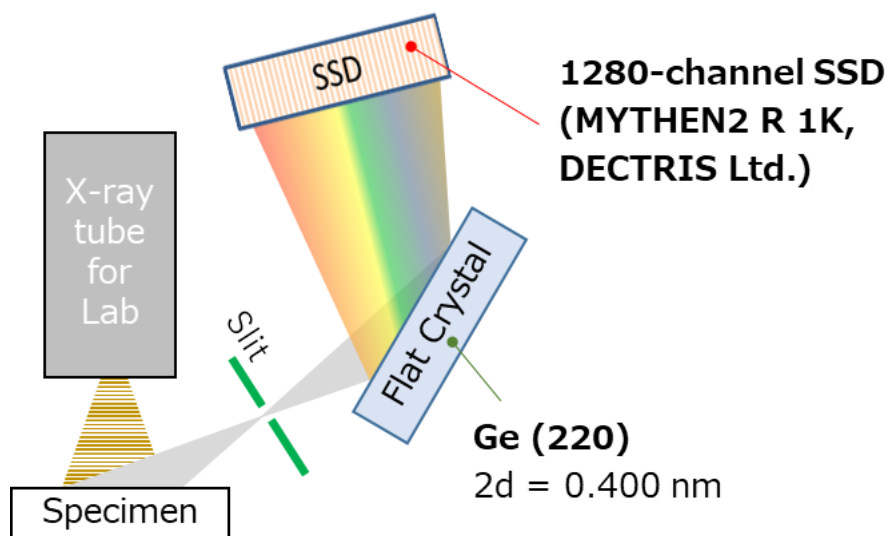


Figure 1. Schematic image of the PS-WDXRF. The detected signals at each channel provide intensity information at different energies.

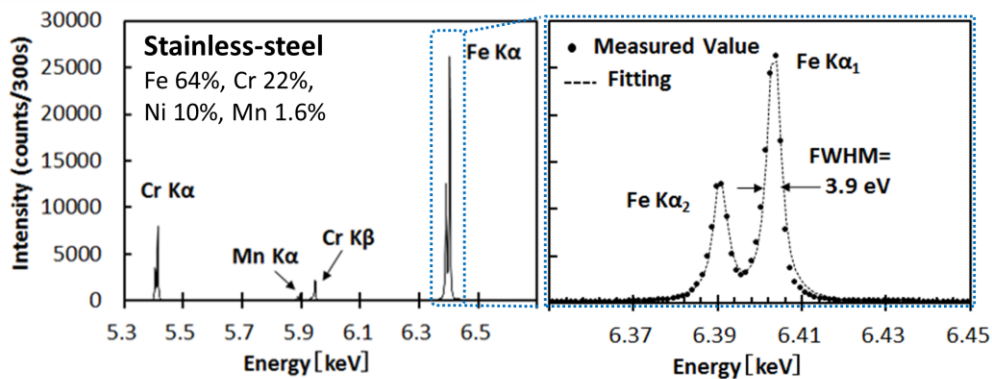


Figure 2. PS-WDXRF spectrum of a stainless-steel ST23. An X-ray within the energy range of 5.38 – 6.52 keV is simultaneously detected with 3.9 eV resolution at FWHM. ST23 is mainly composed of Fe 64 %, Cr 22%, Ni 10 %, and Mn 1.6 %, which was purchased from JFE Techno - Research Corp.

EXPERIMENT

The first step was to obtain and analyze the data from pressed powders of manganese oxides, whose diameter is 30mm, in order to confirm the usefulness of the PS-WDXRF for valence estimation. Thus, three different manganese oxides (MnO_x s) and two different lithium manganese oxides (LMO_x s) were placed in the evacuated chamber of the experimental setup, which has a mechanism available to rotate the sample. The ambient temperature was controlled in the range of ± 0.1 °C in order to suppress the thermal contraction and expansion of the spectrometer. The MnO_x s used in this study were MnO (II), Mn_2O_3 (III) and MnO_2 (IV) (Wako Pure Chemical Industries, Ltd.), and LMO_x s were LiMn_2O_4 (III, IV) and Li_2MnO_3 (IV) (Toshiba Manufacturing Co., Ltd.). An X-ray tube voltage of 20 kV and a current of 100 mA were applied, the target was made from Rh and no primary filter was used. The measurement time was 5 min for MnO_x s and 10 min for LMO_x s. The measurements were repeated five times for each sample while rotating, and then the standard deviation was calculated.

The second step was to correlate the state of charge (SOC) of an actual lithium-ion pouch battery cell with the mean valence state of the manganese in the cathode with PS-WDXRF. Five pouch battery cells based on lithium manganese oxides were prepared. The cell components are shown in Table 1. After the first full charge/discharge cycle, the cells were either partially charged to different SOC values (uncharged: SOC-0, half charged: SOC-50, fully charged: SOC-100), or fully charged and then partially discharged to different depths of discharge (DOD) in the 2nd

cycle (half discharged: DOD-50, and fully discharged: DOD-100). The charge and discharge operations were performed at an ambient temperature of 30 °C with a rate of 0.1 C (current set such that a 10-hour period would be required to change from full-discharged state to full-charged state). The cut off voltage range was controlled from 3.0 to 4.5 V.

Table 1. The pouch battery cell components based on lithium manganese oxides

| | |
|-------------|--|
| Cathode | 90 wt% LiMn ₂ O ₄ 5 wt% acetylene black 5 wt% polyvinylidene difluoride Coating thickness: 50 μm Al current collector: 20 μm |
| Separator | Glass filter (GA100: 430 μm) Celgard (#2325: 25μm) |
| Electrolyte | 1 M LiPF ₆ Ethylene carbonate/diethyl carbonate = 1:1 (vol%) 1 wt% vinylene carbonate |
| Anode | Li Cu current collector Thickness: 500 μm |

After setting the SOC/DOD for each cell, cathodes on aluminum current collectors were harvested from each by carefully disassembling the pouches, as shown in Figure 3, rinsing with DMC (dimethyl carbonate) to remove residual electrolyte and individually laminating each cathodes between sheets of pouch material. These five laminated cathodes were placed in the evacuated chamber of the experimental setup, which has a rotation mechanism available to rotate the sample. The ambient temperature was controlled within ± 0.1 °C. XRF was collected from each cathode sample using a Rh X-ray tube set to a voltage of 20 kV and a current of 100 mA with no primary filter. The X-ray irradiated area is 30 mm in diameter. The measurement time was 10 min. The sample was rotated during the measurement in order to reduce the influence of sample heterogeneity.

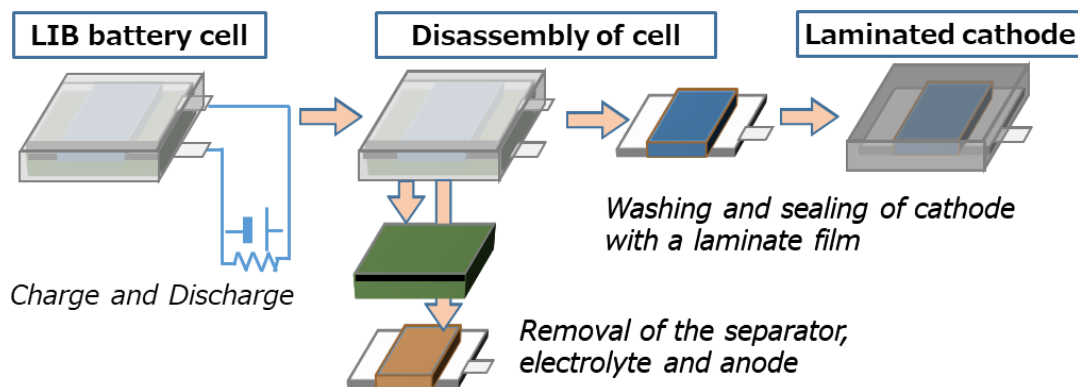


Figure 3. Schematic image of sample preparation method for laminated cathode.

RESULTS AND DISCUSSION

The PS-WDXRF analysis of the different manganese oxides indicates that the specimens produced XRF $K\beta$ peaks at distinct peak energies and shapes as described in Figures 4(a) and 4(b). The $K\beta'$ line, which is one of the satellite $K\beta$ lines obtained from MnO_2 , is broader and weaker than that obtained from MnO . The obtained spectra were well fitted with two Lorentzian peaks, $K\beta_{1,3}$ and $K\beta'$, via the least square algorithm. This energy resolution is achievable by the combination of the instrumental resolution with the fitting precision. Longer measurement time or more peak counts will provide higher fitting precision. The fitted peak energy of the $K\beta_{1,3}$ line obtained from MnO_2 is shifted to lower energies than that obtained from MnO . This shows that the PS-WDXRF has sufficient energy resolution to observe valence information based on the peak energy shift derived from the chemical shift effect (Kawai *et al.*, 1990; Sakurai and Eba, 2003). As plotted in Figure 4(c), the peak energies of Mn $K\beta_{1,3}$ has a high negative correlation with valence number. Moreover, considering that the peak energy difference between MnO and MnO_2 (763 meV, from Table 2) is much larger than the energy-identification precision σ (the standard deviation of the fitted peak energy using the least square algorithm, ~ 21 meV, also from Table 2), the reliability of the valence evaluation is proved. These results indicate that the PS-WDXRF has the potential for valence evaluation of manganese cathode materials with high precision. The ability to determine peak positions with such high precision is the result of the use of a single crystal with a narrow Darwin width to disperse the XRF signal onto the pixels of the detector to give >10 data points within the peak profiles.

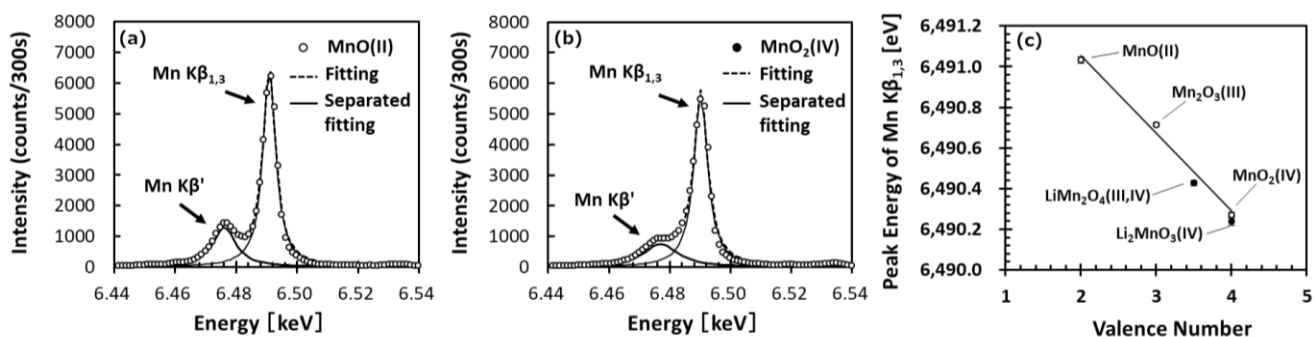


Figure 4. (a) Kβ line of MnO (II). (b) Kβ line of MnO₂ (IV). (c) Valence number vs. Peak Energy of Mn Kβ_{1,3}.

Table 2. Mean peak energy and standard deviation of five times measurement at Mn Kβ_{1,3} line with different oxidization states.

| Specimen | Mean peak energy of Mn Kβ _{1,3} [eV] | Standard deviation [eV] |
|--|---|-------------------------|
| MnO (II) | 6491.033 | 0.015 |
| Mn ₂ O ₃ (III) | 6490.715 | 0.008 |
| MnO ₂ (IV) | 6490.270 | 0.015 |
| LiMn ₂ O ₄ (III, IV) | 6490.428 | 0.012 |
| Li ₂ MnO ₃ (IV) | 6490.240 | 0.021 |

The resulting peak energies of Mn Kβ_{1,3} in the harvested cathodes are given in Table 3 and plotted in Figure 5(a), which shows that the peak shifts to lower energy during charge and higher energy during discharge. The valence conversion from the peak energy of Mn Kβ_{1,3} was performed with respect to the reference valence numbers of LiMn₂O₄ (III, IV) and Li₂MnO₃ (IV). As shown in Figure 5(b) plotted from Table 4, the valence number of the LIB manganese cathode material changed from approximately 3.9 at the charged (delithiated) state to around 3.5 at the discharged (lithiated) state.

Table 3. Mean peak energy and standard deviation of five measurements of the cathode material at Mn Kβ_{1,3} line with different state of charge (SOC) and depth of discharge (DOD)

| State of charge/discharge | Mean peak energy of Mn Kβ _{1,3} [eV] | Standard deviation [eV] |
|---------------------------|---|-------------------------|
| SOC-0 | 6490.407 | 0.025 |
| SOC-50 | 6490.357 | 0.018 |
| SOC-100 | 6490.304 | 0.034 |
| DOD-50 | 6490.364 | 0.013 |
| DOD-100 | 6490.419 | 0.023 |

Table 4. Mean valence and standard deviation of five measurements of the cathode material with different state of charge (SOC) and depth of discharge (DOD)

| State of charge/discharge | Mean valence (converted from LiMn ₂ O ₄ and Li ₂ MnO ₃) | Standard deviation |
|---------------------------|--|--------------------|
| SOC-0 | 3.55 | 0.065 |
| SOC-50 | 3.69 | 0.048 |
| SOC-100 | 3.83 | 0.092 |
| DOD-50 | 3.67 | 0.035 |
| DOD-100 | 3.52 | 0.063 |

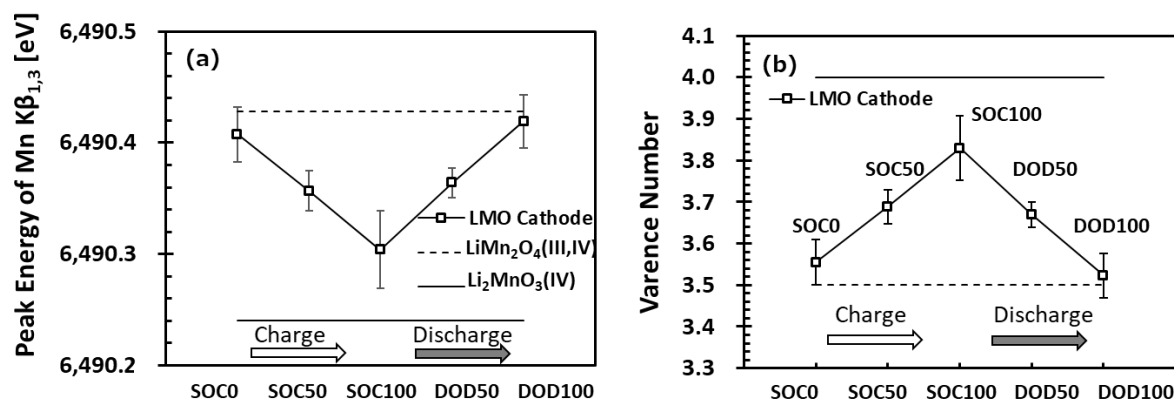
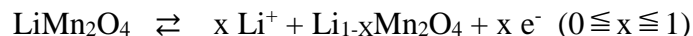


Figure 5. (a) Plot of the peak energies of Mn Kβ_{1,3} at each SOC and DOD. (b) Converted valence number plot from the peak energies of Figure 5(a).

In manganese-based LIBs with spinel LiMn₂O₄ as the cathode active material, the mean valence of the Mn is expected to vary between 3.5 and 4.0 by charging and discharging (Xia and Yoshio, 1996). The electrochemical reaction of this cathode material is shown in below.



The result shown in Figure 5(b) is in good accordance with this reaction formula.

CONCLUSION

Fitting peaks from PS-WDXRF achieves high energy-identification precision of approximately 20 meV. The precision is sufficient for the valence evaluation of LIB cathodes. In ex-situ examination of LIB cathodes using the PS-WDXRF measurement, we estimate that the mean valence state of the manganese cathode material varied from about 3.9 in the charged state (delithated cathode) to 3.5 in the discharged state (lithiated cathode), which is in good accordance with the reaction formula. The PS-WDXRF achieves high energy-identification precision through a combination of a single crystal reflection with a narrow Darwin width and a position-sensitive detector, which can be configured to collect a sufficient number of points across an XRF peak to enable fitting with uncertainties well below the instrumental resolution. Although each peak is measured in a single static configuration, the system can be reconfigured as needed for each element analyzed. The PS-WDXRF is a powerful tool for the chemical valence evaluation in the laboratory and can be applied to important problems, such as the evaluation of the state of lithiation of cathode materials for LIBs studies.

REFERENCES

- Sato, K., Nishimura, A., Kaino, M., and Adachi, S. (2017). "Polychromatic simultaneous WDXRF for chemical state analysis using laboratory X-ray source," *X-Ray Spectrom.*, **46**, 330-335.
- Kawai, J., Takami, M., and Satoko, C. (1990). "Multiplet Structure in Ni $K\beta$ X-ray fluorescence spectra of nickel compounds," *Phys. Rev. Lett.*, **65**, 2193–2196.
- Sakurai, K. and Eba, H. (2003). "Chemical characterization using relative intensity of manganese $K\beta'$ and $K\beta_5$ X-ray fluorescence," *Nucl. Instr. and Meth. in Phys. Res.*, **B199**, 391–395.
- Xia, Y. and Yoshio, M. (1996). "An Investigation of Lithium Ion Insertion into Spinel Structure Li - Mn - O Compounds," *J. Electrochem. Soc.*, **143**, 825–833.